

Supplemental Information

SUPPLEMENTAL METHODS

Ultrastructure studies

From mice killed via cervical dislocation the heart was rapidly removed and small (~1-2 mm³) pieces of the left ventricular free wall were immersion-fixed in Karnovsky's fixative. The fixed samples were stained *en block* with partially reduced osmium tetroxide (0.8% potassium-ferrocyanide and 2% osmium tetroxide in 0.1 M sodium cacodylate buffer overnight at 4°C) and in turn with 1% uranyl acetate (1hr at 4°C). Stained samples were dehydrated on an acetone dilution series and embedded in Spurr's resin according to manufacturer's (Electron Microscopy Sciences) instructions. 60-100 nm thin sections were cut from the embedded specimens, mounted on electron microscopy grids and examined using a FEI Tecnai 12 TEM equipped with a phosphor plate (Advanced Microscopy Techniques, AMT) and Hamamatsu Orca 8Mpx digital camera.

Morphometric analysis of mitochondria and the SR-mitochondrial associations was carried out on longitudinal sections using MacBiophotonics' Image J software. For the generic characterization of mitochondrial morphology and abundance, a mask was drawn over the largest possible sarcoplasmic area (without subsarcolemmal and perinuclear regions) in a cardiomyocyte section, and under this mask for each mitochondrial cross sections the area, perimeter and the major axis of the fitted ellipse were determined. The percent of the sarcoplasmic area covered by mitochondria was used as the 2D equivalent of mitochondrial volume density. The number of individual mitochondrial cross sections per 10 μm² was also determined that together with the mitochondrial density reflected on the fusion/fragmentation states.

For the morphometric analysis of SR-mitochondrial associations a comprehensive protocol is yet to be established. Most of the published TEM analyses focus on the distance between the interfacing mitochondrial and SR membranes¹ or T-tubule centers². However, as the platforms for local functional crosstalk, besides their tightness the extent of these associations is just as important in a comparative analysis. We have introduced a protocol in this regard for the analysis of ER-mitochondrial associations in non-muscle cells in 2006³ that we adopted now for the quantification of SR-mitochondrial associations in the cardiac muscle as follows. Areas where the junctional SR (jSR) was <50 nm away from the outer mitochondrial membrane were accounted as jSR-mitochondrial interfaces. Since the SR-derived Ca²⁺ signals that locally propagate to the mitochondria in the ventricular muscle are generated mainly in the T-tubule SR junctions (dyads), the analysis was restricted to the intermyofibrillar mitochondria (excluding the distinct sub-sarcolemmal and perinuclear mitochondrial population). This restriction also applied to the generic mitochondrial parameters. The dyad-forming SR regions are the terminal cisternae (jSR) that are localized to the Z disks and so they mostly associate with the transversal side of the mitochondrion, while the longitudinal sides are enmeshed by the network SR^{4, 5}. Hence, to reference the extent of jSR-mitochondria associations we chose to quantify the length of the mitochondrial interface as the fraction of the participating mitochondrial transversal side (100 % meaning a transversal side fully covered by jSR). Importantly, the length of these transversal sides was not different between Mfn1^{-/-} and Mfn2^{-/-} and their respective control samples (Fig. 4b and 4c). For the SR-mitochondrial gap distance for each associations 3-5 individual distance readings (evenly distributed over the interface length) were averaged. For the cumulative analysis, each contributing mitochondrion was represented by a single distance

number. If a mitochondrion (transversal side) had more than one jSR association, a weighted average (based on surface representation) was created from the distance values of these associations.

L-type Ca²⁺ channel electrophysiological recordings

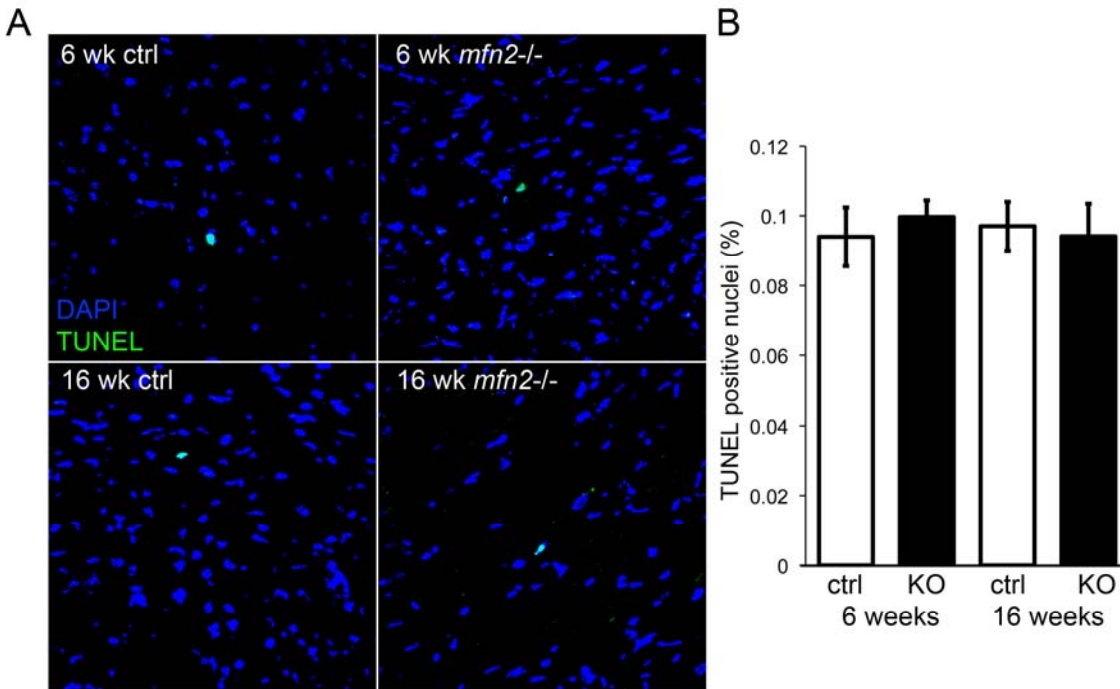
Whole-cell recordings were obtained from LV myocytes within 12h of isolation at room temperature. Experiments were performed using a Dagan 3900A (Dagan Corporation, Minneapolis, MN, USA) patch clamp amplifier interfaced to a microcomputer with a Digidata 1332 analog/digital interface and the pCLAMP9 software package (Molecular Devices). Data were filtered at 5 kHz before storage. For recordings of whole-cell Ca²⁺ currents (I_{CaL}), pipettes contained (in mM): CsCl 135; EGTA 10; HEPES 10; glucose 5.5; MgATP 3 and TrisGTP 0.4 (pH 7.2; 310 mOsm). The bath solution contained (in mmol/L): TEACl 140; KCl 4; MgCl₂ 2; CaCl₂ 2; HEPES 10 and glucose 10 (pH 7.4; 310mOsm). Currents were evoked in response to 400 ms voltage steps to test potentials between -40 and +50 mV from a holding potential (-40 mV) to inactivate voltage-gated Na⁺ currents. Data were compiled and analyzed using Clampfit (Version 9.2, Molecular Devices) and Excel (Microsoft, Redmond, WA, USA). Integration of the capacitive transients, recorded during brief ± 10 mV voltage steps from the holding potential (-70 mV), provided the whole-cell membrane capacitance (C_m). Leak currents were always <100 pA, and were not subtracted. Series resistances (<10 M Ω) were routinely compensated electronically (>80%). Voltage errors resulting from the uncompensated series resistances were ≤ 8 mV and were not corrected. Peak I_{CaL} amplitudes were measured and normalized to whole-cell membrane capacitances (in the same cell) and current densities (in pA/pF) were compared.

Patch clamp solutions

Solutions used in patch-clamp and field-stimulation experiments (Figure 5; Supplemental Figures III, IV):

- **Normal Tyrode's** (perfusion) solution containing (in mmol/L): NaCl 130, KCl 5, MgCl₂ 1, CaCl₂ 2, Na-HEPES 10, glucose 10, Na-pyruvate 2 and ascorbic acid 0.3, pH 7.4.
- **Pipette solution** (in mmol/L): K-glutamate 130, KCl 19, MgCl₂ 0.5, Na-HEPES 15, Mg-ATP 5, pH 7.2.

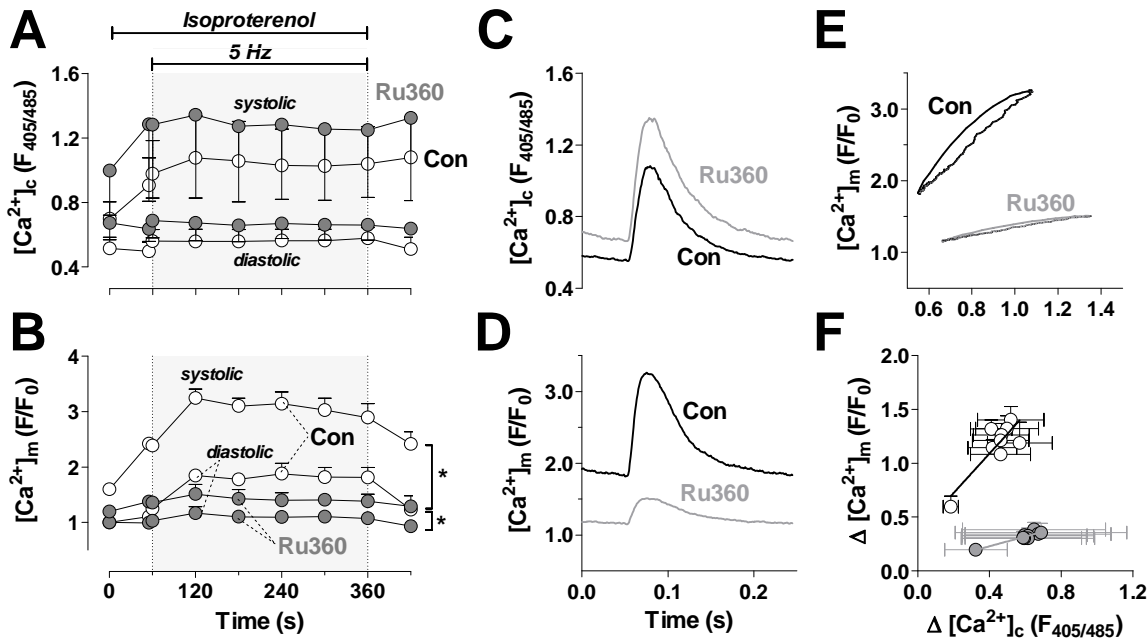
SUPPLEMENTAL FIGURES



Online Figure I.

TUNEL labeling of Mfn2 KO hearts.

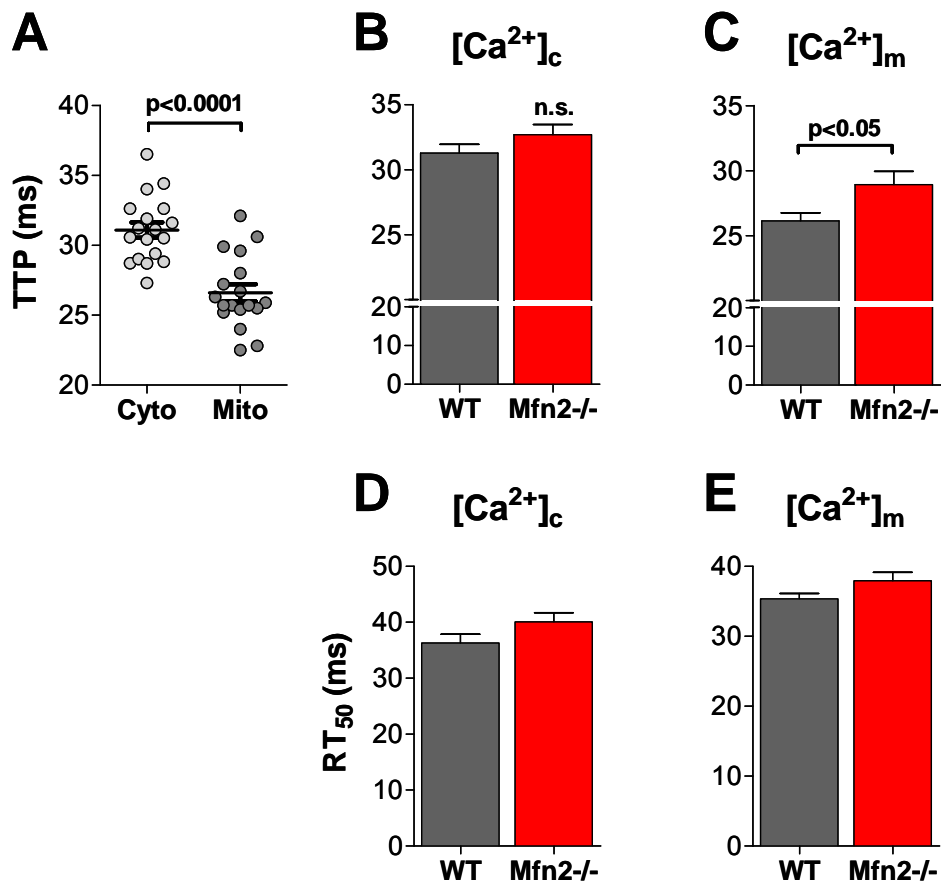
A. Representative TUNEL labeling fluorescent micrographs of control and Mfn2 KO cardiac sections at 6-week and 16 weeks of age. Green: TUNEL positive labeling; Blue: DAPI nuclear counterstain. **B.** Quantitative TUNEL analysis ($n = 5$ per group).



Online Figure II:

Ru360 inhibits mitochondrial, but not cytosolic Ca^{2+} transients and accumulation.

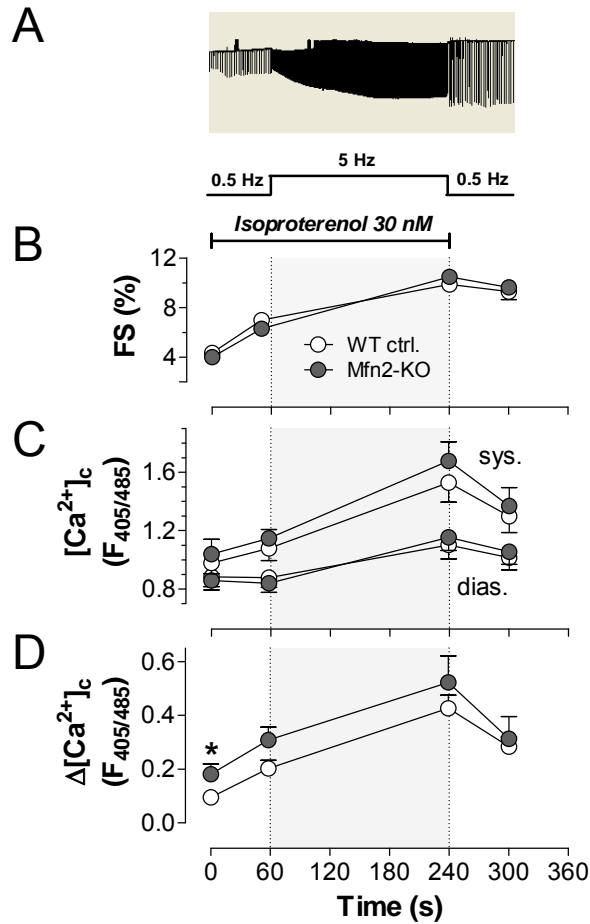
Recordings of $[Ca^{2+}]_c$ (**A, C**) and $[Ca^{2+}]_m$ (**B, D**), determined by indo-1 and rhod-2, respectively, in patch-clamped cardiac myocytes (from C57BL/6N mice) exposed to a protocol of 0.5 Hz voltage-clamp depolarizations and an increase to 5 Hz (grey areas) in the presence of isoproterenol. The pipette solution contained the MCU-inhibitor Ru360 (1 μ M) or vehicle (Control), respectively. The data of the whole protocol (**A, B**) or averaged transients at 120 s (isoproterenol) are given. **E** and **F**, $[Ca^{2+}]_m$ plotted against $[Ca^{2+}]_c$ for single transients (at 5 Hz, 120 s; **E**) or as averaged values for the entire experiment (**F**) in the absence and presence of Ru360. * $p < 0.05$ (ANOVA for repeated measures).



Online Figure III:

Cytosolic and mitochondrial Ca^{2+} upstroke and decay kinetics in Mfn2-KO and WT myocytes.

A, Time-to-peak (TTP) of cytosolic and mitochondrial Ca^{2+} transients in all WT myocytes. **B** and **C**, TTP of $[Ca^{2+}]_c$ (**B**) and $[Ca^{2+}]_m$ (**C**) in WT and Mfn2-KO myocytes, respectively. **D** and **E**, Time to 50% decay of $[Ca^{2+}]_c$ (**D**) and $[Ca^{2+}]_m$ (**E**) in WT and Mfn2-KO myocytes, respectively. Data were obtained at steady-state 5 Hz stimulation in the presence of isoproterenol.



Online Figure IV.

Cardiomyocyte bioenergetic stress response studies.

Murine adult ventricular myocytes undergoing field-stimulation at 0.5 Hz were exposed to isoproterenol (30 nM) and stimulation frequency was subsequently increased to 5 Hz for 3 min.

A. Original trace of sarcomere shortening recordings with time course matched to the data sets in panels B, C and D, Figure 5 E and F. Fractional sarcomere shortening (**B**; FS), systolic and diastolic [Ca²⁺]_c (**C**) and amplitude of [Ca²⁺]_c transients (**D**) for Mfn2^{-/-} (control and KO), respectively. n=30-50 cells for sarcomere shortening and 6-12 cells for Ca²⁺ studies. *p<0.05.

SUPPLEMENTAL TABLE

Online Table I. Genotypes of *Mfn1* and *Mfn2* cardiac KO crosses.

Genotype	Observed total	Expected F/F x Cre	Observed F/F x Cre
<i>mfn1</i> x <i>Myh6</i> -Cre	n=103	n=52	n=53
<i>mfn2</i> x <i>Myh6</i> -Cre	n=298	n=149	n=138

Homozygous *mfn* floxed mice (*mfn*^{loxp/loxp}; F/F) were bred to mice homozygous for the same floxed *mfn* allele and heterozygous for either *Myh6*-CRE. There were no differences between observed and expected (Chi square test).

Supplemental References

1. Franzini-Armstrong C. ER-mitochondria communication. How privileged? *Physiology (Bethesda)*. 2007;22:261-268.
2. Papanicolaou KN, Khairallah RJ, Ngoh GA, Chikando A, Luptak I, O'Shea KM, Riley DD, Lugus JJ, Colucci WS, Lederer WJ, Stanley WC, Walsh K. Mitofusin-2 maintains mitochondrial structure and contributes to stress-induced permeability transition in cardiac myocytes. *Mol Cell Biol*. 2011;31:1309-1328.
3. Csordas G, Renken C, Varnai P, Walter L, Weaver D, Buttle KF, Balla T, Mannella CA, Hajnoczky G. Structural and functional features and significance of the physical linkage between ER and mitochondria. *J Cell Biol*. 2006;174:915-921.
4. Yoshikane H, Nihei T, Moriyama K. Three-dimensional observation of intracellular membranous structures in dog heart muscle cells by scanning electron microscopy. *J Submicrosc Cytol*. 1986;18:629-636.
5. Segretain D, Rambourg A, Clermont Y. Three dimensional arrangement of mitochondria and endoplasmic reticulum in the heart muscle fiber of the rat. *Anat Rec*. 1981;200:139-151.

Circulation Research [Print Close](#)

LWW Cover Sheet for CIRCRESAHA/2012/266585

Manuscript Number: 266585-R2	Date original received:	<input type="text" value="02/06/2012"/>	Print issue date: <input type="text" value="08/31/2012"/>
Article Type: Regular Article	Date most recent revision received:	<input type="text" value="06/25/2012"/>	Print cover date: <input type="text" value="08/31/2012"/>
Handling editor: Houser	Date resubmission received:	<input type="text"/>	Online publication date: <input type="text" value="07/09/2012"/>
Is handling editor a consulting editor? <input type="radio"/> yes <input checked="" type="radio"/> no	Date most recent revised resubmission received:	<input type="text"/>	# of Pages: <input type="text" value="17"/>
Thematic review article text box needed? <input type="radio"/> yes <input checked="" type="radio"/> no	Accepted: <input type="text" value="07/09/2012"/>	Page Overage Charges: <input type="text" value="\$425"/>	
	To Cadmus: <input type="text" value="07/09/2012"/>		

Authors: Yun Chen, György Csordás, Casey Jowdy, Timothy G. Schneider, Norbert Csordás, Wei Wang, Yingqiu Liu, Michael Kohlhaas, Maxie Meiser, Stefanie Bergem, Jeanne M. Nerbonne, Gerald W. Dorn II, and Christoph Maack

Title: Mitofusin 2-containing Mitochondrial-Reticular Microdomains Direct Rapid Cardiomyocyte Bioenergetic Responses via Inter-Organellar Ca²⁺ Crosstalk

Subject codes: [136] [140] [107]

Figures and Tables

Tables:

Figures:

Figure legends:

Color Figures: yes no
 Hard Copy Electronic

Halftone Figures: yes no
 Hard Copy Electronic

Online Data Supplement

yes no

File Type:

pdf

video files

other

Copyright/Acknowledgments

Copyright transfer agreement complete: yes no

Conflict of interest disclosure complete: yes no

Citation of research support: yes no

Acknowledgment permissions: yes no n/a

Corresponding Author Information

Dr. Christoph Maack
 Universitätsklinikum des Saarlandes
 Klinik für Innere Medizin III
 Gebäude 40
 Homburg/Saar, Germany
 66424
 Tel: +49-(0)6841-1621380
 Fax: +49-(0)6841-1623434
 Email: maack@gmx.org